occupies a special position on a twofold axis; K(2) is at a general position. Both types of K atoms are surrounded by ten O atoms. The K—O distances in each coordination polyhedron are shown by dotted lines in Fig. 1. The K—O distances in each KO_{10} polyhedron in TKHSe are more scattered than those in TRHSe and TRDSe.

The two SeO_4 groups in the dimer are related by a centre of symmetry, at which the H atom is located or positionally disordered. The large B value of the H atom appears to favour the disordering (Table 2). The dimensions and systematic trends in distortion from a regular tetrahedron of the SeO_4 anion, as shown from the bond lengths and angles, are close to those in TRHSe and TRDSe [for detailed discussion consult Ichikawa *et al.* (1992*a*)]. Furthermore, a trend among the values of the equivalent isotropic displacement parameters and the disk-like anisotropy in the O(2)(H) and O(3) atoms are similarly observed in the Rb and Cs analogues [see the deposited list of anisotropic displacement parameters and Ichikawa, Gustafsson & Olovsson (1992*b*)].

The hydrogen-bond distance $O(2)\cdots O(2^{ii})$ is 2.524 (5) Å. This value is the shortest among the members of the $M_3H(SeO_4)_2$ family exhibiting a low-temperature phase transition. That also means that $K_3H(SeO_4)_2$ with the shortest hydrogen bond has the lowest transition temperature. We thus expect that a linear relation between the transition temperature and hydrogen-bond distance at T_c is also valid for the $M_3H(SeO_4)_2$ family (Ichikawa, Motida & Yamada, 1987). Structure analysis at 30 K is now in progress, which will give us the definite conclusion to the validity of the linear correlation.

References

BARANOV, A. I., TREGUBCHENKO, A. V., SHUVALOV, L. A. & SHCHAGINA, N. M. (1987). *Sov. Phys. Solid State*, **29**, 1448–1449.
ENDO, M., KANEKO, T., OSAKA, T. & MAKITA, Y. (1983). *J. Phys. Soc. Jpn*, **52**, 3829–3832.
ICHIKAWA, M., GUSTAFSSON, T. & OLOVSSON, I. (1991). *Solid State Commun.* **78**, 547–551.
ICHIKAWA, M., GUSTAFSSON, T. & OLOVSSON, I. (1992*a*). *Acta Cryst.* **C48**, 603–607.
ICHIKAWA, M., GUSTAFSSON, T. & OLOVSSON, I. (1992*b*). *Acta Cryst.* B48. In the press.
ICHIKAWA, M., MOTIDA, K. & YAMADA, N. (1987). *Phys. Rev. B*, **36**, 874–876.
JOHNSON, C. K. (1976). *ORTEP*II. Report ORNL-5138. Oak Ridge National Laboratory, Tennessee, USA.
LUNDGREN, J.-O. (1983). *Crystallographic Computer Programs.* Report UUIC-B13-4-05. Institute of Chemistry, Univ. of Uppsala, Sweden.
MCCANDLISH, L. E., STOUT, G. H. & ANDREWS, L. C. (1975). *Acta Cryst.* A31, 245–249.
MERINOV, B. V., BARANOV, A. I. & SHUVALOV, L. A. (1990). *Sov. Phys. Crystallogr.* **35**, 200–203.

A Neutron Powder Diffraction Study of HIO₃ and DIO₃

BY KENNY STÅHL

Inorganic Chemistry 2, University of Lund, POB 124, S-221 00 Lund, Sweden

AND MAREK SZAFRANSKI

Institute of Physics, Adam Mickiewicz University, Grunwaldzka 6, P-60-780 Poznań, Poland

Abstract. The crystal structures of hydrogen iodate, HIO_3, and its deuterated form, DIO_3, have been refined using the Rietveld method from neutron powder-diffraction data; $\lambda = 1.470$ (1) Å, $T = 295$ K, $P2_12_12_1$, $Z = 4$; HIO_3: $M_r = 175.91$, $a = 5.5448$ (3), $b = 5.8829$ (3), $c = 7.7434$ (4) Å, $V = 252.59$ (4) Å³, $D_x = 4.64$ g cm⁻³, $\mu = 0.72$ cm⁻¹, $9 \leq 2\theta \leq 118.7°$ in 1372 steps, $R_p = 1.51\%$, $R_{wp} = 1.92\%$, GOF = 1.38, $R_F = 0.32\%$ (274 Bragg reflections) and 36 refined parameters; DIO_3: $M_r = 176.91$, $a = 5.5408$ (4), $b =$

5.8745 (4), $c = 7.7356$ (5) Å, $V = 251.79$ (5) Å^3, $D_x = 4.67$ g cm^{-3}, $\mu = 0.06$ cm^{-1}, $10 \le 2\theta \le 128°$ in 1475 steps, $R_p = 4.64\%$, $R_{wp} = 6.17\%$, GOF = 5.92, $R_F = 1.50\%$ (307 Bragg reflections) and 37 refined parameters. The iodate group forms a pyramid with I as one apex. H/D forms rather linear O—H/D⋯O hydrogen bonds with O—H 0.968 (9) and O—D 1.009 (7) Å. With the inclusion of next-nearest neighbours at distances 2.5 to 3.5 Å, the I—O coordination can be described as a capped trigonal prism, with I approximately on the capped face of the prism. The H/DIO₃ structures are of the *anti*-cementite type, with H/D in one face of the octahedral interstices (empty in cementite) and with the I-atom lone pair approximately at the centre of the prisms (the cementite C position).

Introduction. The crystal structure of HIO₃ has previously been determined by Rogers & Helmholz (1941) (X-rays) and Garret (1954) (neutrons, 0*kl* and *h*0*l* zones, Fourier refinement). Modelling of the optical and spectroscopic properties of HIO₃ and DIO₃ (Szafranski, 1991) raised the need for more accurate structural data. The present study is an attempt to obtain this from neutron powder-diffraction data. It is the first least-squares refinement of the HIO₃ structure and the first structural study of DIO₃ reported.

Experimental. The HIO₃ sample used was commercially available AnalaR quality, BDH Chemicals Ltd, Poole, England. DIO₃ was obtained from five-times-repeated recrystallizations through slow evaporation at 323 K from D₂O with addition of DNO₃, starting with HIO₃. The samples were ground and packed through vibrations in an ultrasonic bath in a vanadium sample container of 11 mm diameter and 50 mm height. Both data sets were collected at the powder diffraction beam line at The Studsvik Neutron Research Laboratory, Sweden. The wavelength, 1.470 (1) Å, was obtained using a Cu(220) double-crystal monochromator, calibrated with Al₂O₃. The diffractometer is built on a Huber $\omega/2\theta$ goniometer, operating in parallel mode, equipped with an array of ten ³He detectors, 3.12° apart, and with 10′ Soller slits in front. The data sets were collected at ambient pressure and temperature in 2θ step sizes of 0.08°, each step measured for approximately 2 min (monitor controlled) without sample rotation.

The Rietveld analysis program used in this study is essentially the *LHMP*1 program described by Hill & Howard (1986) modified to fit the local I/O formats. The program minimizes the quantity $\sum w_i(Y_{io} - Y_{ic})^2$ with $w_i = 1/Y_{io}$. Pseudo-Voigt functions were used in both refinements with a Lorentzian component $\gamma = \gamma_1 + \gamma_2 2\theta$, where γ_1 (HIO₃ and DIO₃) and γ_2 (DIO₃)

were refined. The FWHM is defined as $(U\tan^2\theta + V\tan\theta + W)^{1/2}$, where U, V and W were refined using a peak width of five half widths. The 2θ zero point and six background parameters $[B_i = \sum B_{im}(2\theta)^m, m = -1, 0, 1, 2, 3, 4]$ were refined as well as one asymmetry parameter for $2\theta \le 30°$ (HIO₃) and one preferred-orientation parameter (DIO₃). The data sets were corrected for absorption according to Rouse, Cooper, York & Chakera (1970), giving maximum corrections of 1.40 (HIO₃) and 1.04 (DIO₃). One overall scale factor, three unit-cell parameters and fractional coordinates and isotropic temperature factor coefficients of all atoms were refined for both data sets. The refinements were started with parameters from Garret (1954). Neutron scattering lengths were taken from Koester, Rauch, Herkens & Schroeder (1981). The maximum shift/ e.s.d. in the final cycle was less than 0.1 in both refinements. On introduction of anisotropic temperature factor coefficients the refinements converged to $R_{wp} = 1.82\%$ and 5.52% for HIO₃ and DIO₃ respectively. The anisotropic model, with 25 more parameters, cannot be rejected on the 0.005 level according to the Hamilton R-value test (*International Tables for X-ray Crystallography*, 1974, Vol. IV). However, as most of the temperature factors did not become positive definite and e.s.d.'s generally increased, the isotropic model was retained.

R values used are defined as $R_p = \sum|Y_{io} - Y_{ic}|/\sum Y_{io}$, $R_{wp} = [\sum w_i(Y_{io} - Y_{ic})^2]/[\sum w_i Y_{io}^2]^{1/2}$, GOF $= \sum w_i(Y_{io} - Y_{ic})^2/(N - P)$ and the derived Bragg R values, $R_I = \sum|I_{ko} - I_{kc}|/\sum I_{ko}$, $R_F = \sum|F_{ko} - F_{kc}|/\sum F_{ko}$. Additional information on data collections and refinements is given in Table 1, and the final fractional coordinates and isotropic mean values of the temperature factor coefficients are given in Table 2. The powder diffraction patterns with their final difference patterns are shown in Fig. 1.*

Discussion. The geometric details of the HIO₃ and DIO₃ structures are given in Table 3 and compared to those found by Garret (1954). The iodate ion forms a pyramid with the I-atom lone pair pointing at the fourth vertex of a tetrahedron. With inclusion of next-nearest neighbours at distances 2.50–3.50 Å, the I—O coordination can be described as a distorted capped trigonal prism, with the I atom approximately on the capped prism face. The HIO₃ and DIO₃ structures are of the *anti*-cementite type (Hyde & Andersson, 1989), related to the NaIO₃

Table 1. *Data collection and refinement data for* HIO_3 *and* DIO_3

Space group $P2_12_12_1$, $Z = 4$.

	HIO_3	DIO_3
Maximum $\sin\theta/\lambda$ (Å^{-1})	0.585	0.612
Number of steps	1372	1475
Number of Bragg peaks	274	307
Number of parameters refined	36	37
a (Å)	5.5448 (3)	5.5408 (4)
b (Å)	5.8829 (3)	5.8745 (4)
c (Å)	7.7434 (4)	7.7356 (5)
V (Å^3)	252.59 (4)	251.79 (5)
R_p (%)	1.51	4.64
R_{wp} (%)	1.92	6.17
GOF	1.38	5.92
R_I (%)	0.61	3.68
R_F (%)	0.32	1.50

Table 2. *Final fractional coordinates* ($\times 10^4$) *and isotropic temperature factor coefficients* (Å^2) *for* HIO_3 *and* DIO_3

	x	y	z	B
HIO_3				
I	2028 (8)	−858 (7)	1576 (5)	0.3 (1)
O(1)	−674 (7)	237 (6)	2552 (6)	1.0 (1)
O(2)	3338 (7)	1960 (8)	839 (6)	1.2 (1)
O(3)	963 (8)	−1591 (6)	−527 (5)	0.8 (1)
H	2419 (12)	3198 (14)	1335 (10)	2.5 (2)
DIO_3				
I	2042 (10)	−902 (9)	1574 (7)	0.6 (1)
O(1)	−686 (9)	234 (7)	2565 (9)	0.8 (1)
O(2)	3385 (8)	1927 (9)	834 (6)	0.6 (1)
O(3)	997 (9)	−1599 (8)	−534 (6)	0.4 (1)
D	2361 (10)	3175 (8)	1349 (7)	3.2 (2)

Table 3. *Selected distances* (Å) *and angles* (°) *in* HIO_3 *and* DIO_3

	HIO_3	DIO_3	HIO_3 (Garret, 1954)
I—O(1)	1.797 (6)	1.821 (7)	1.820 (11)
I—O(2)	1.898 (6)	1.909 (7)	1.900 (11)
I—O(3)	1.786 (6)	1.778 (7)	1.779 (11)
I—O(1^i)	2.509 (5)	2.482 (7)	2.501 (11)
I—O(2^{ii})	3.501 (6)	3.474 (7)	3.475 (10)
I—O(3^{iii})	2.770 (6)	2.758 (7)	2.770 (10)
I—O(3^{iv})	2.889 (6)	2.889 (7)	2.882 (11)
O(1)—I—O(2)	97.6 (2)	97.5 (3)	97.6 (5)
O(1)—I—O(3)	101.2 (3)	101.6 (4)	100.7 (5)
O(2)—I—O(3)	93.6 (3)	93.0 (3)	93.8 (5)
O(2)—H/D	0.968 (9)	1.009 (7)	0.990 (18)
H/D···O(1^v)	1.766 (8)	1.741 (7)	1.702 (18)
O(2)—H/D—O(1^v)	173.2 (8)	174.4 (6)	173.0 (1.5)
I—O(2)—H/D	109.7 (6)	107.1 (5)	108.9 (1.1)

Symmetry code: (i) $-x$, $y - \frac{1}{2}$, $\frac{1}{2} - z$; (ii) $1 - x$, $y - \frac{1}{2}$, $\frac{1}{2} - z$; (iii) $\frac{1}{2} + x$, $-y - \frac{1}{2}$, $-z$; (iv) $\frac{1}{2} - x$, $-y$, $\frac{1}{2} + z$; (v) $-x$, $\frac{1}{2} + y$, $\frac{1}{2} - z$.

structure (Svensson & Ståhl, 1988), with H/D in one face of the octahedral interstice (empty in cementite, occupied by Na in $NaIO_3$) and with the I-atom lone pair near the centre of the prism (cementite C position), *cf.* Fig. 2. The significant differences between

the molecular geometries of HIO_3 and DIO_3 are restricted to the H and D bonds: the O—H distance is 0.041 (11) Å shorter than the O—D distance and the I—O—H angle is 2.6 (8)° larger than the I—O—D angle; the next-nearest-neighbour distances are on average 0.017 (4) Å larger in HIO_3, which is
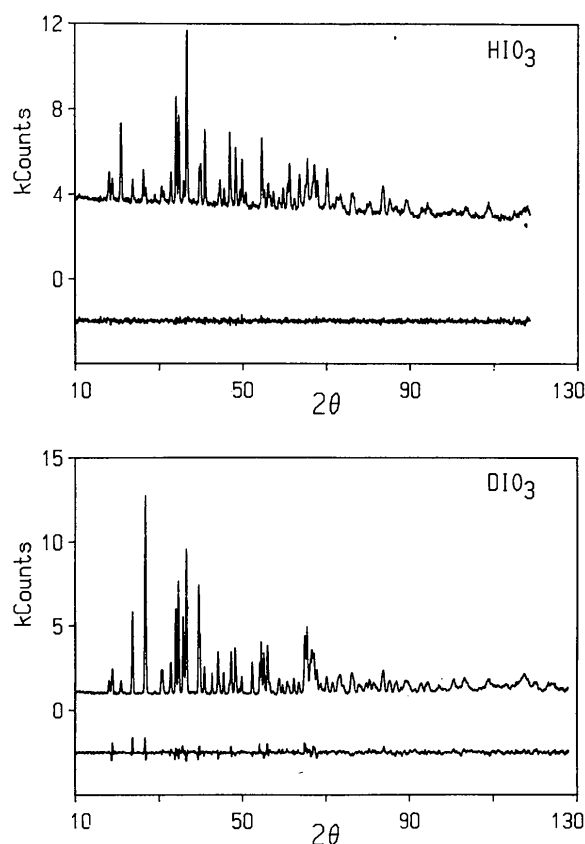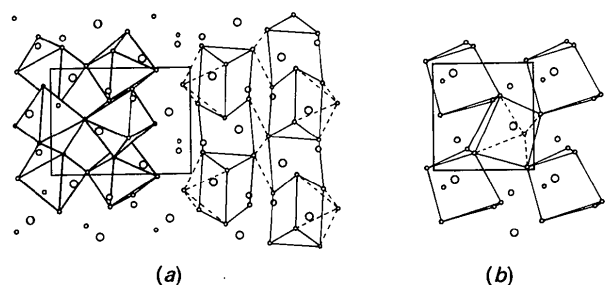

Fig. 1. Diffraction patterns and final difference patterns for HIO_3 and DIO_3.

(a)   (b)

Fig. 2. The crystal structures of HIO_3 and DIO_3. (*a*) Projection on the *bc* plane; to the left the H/DO_6 octahedra and the unit cell; the atomic positions are extended to the right hand side, where the connected capped prisms around I are shown; broken lines indicate capping. (*b*) Projection on the *ab* plane: a view perpendicular to the sheets of connected capped prisms; large circles represent I, intermediate circles H/D and small circles O atoms.

also reflected in the larger HIO$_3$ unit cell. The present results on HIO$_3$ are in agreement with those found by Garret (1954), but at an apparent higher level of precision. However, e.s.d.'s and significance of small differences between results obtained in this study, using the Rietveld method, and those of Garret (1954), using Fourier refinements, have to be treated cautiously owing to the likely underestimate of the e.s.d's by the two methods. In order to further increase the precision in the structure determinations of HIO$_3$ and DIO$_3$, single-crystal neutron diffraction studies will be attempted in the near future.

References

GARRET, B. S. (1954). Report ORNL-1745, pp. 97–148. Oak Ridge National Laboratory, Tennessee, USA.
HILL, R. J. & HOWARD, C. J. (1986). Australian Atomic Energy Commission (now ANSTO) Report M112. Lucas Heights Research Laboratories, New South Wales, Australia.
HYDE, B. G. & ANDERSSON, S. (1989). *Inorganic Crystal Structures*. New York: John Wiley.
KOESTER, L., RAUCH, H., HERKENS, M. & SCHROEDER, K. (1981). KFA Report Jül-1755. Kernforschungsanlage, Jülich, Germany.
ROGERS, M. T. & HELMHOLZ, J. (1941). *J. Am. Chem. Soc.* **63**, 278–284.
ROUSE, K. D., COOPER, M. J., YORK, E. J. & CHAKERA, A. (1970). *Acta Cryst.* **A26**, 682–691.
STÅHL, K. (1990). Studsvik Neutron Research Laboratory Progress Report 1987–1989, pp. 39–40. Univ. of Uppsala, Sweden.
SVENSSON, C. & STÅHL, K. (1988). *J. Solid State Chem.* **77**, 112–116.
SZAFRANSKI, M. (1991). PhD Thesis. Adam Mickiewicz Univ., Poznań, Poland.

Structure of Pentaamminechlororuthenium(III) Bisulfate Tetrahydrate

BY ELIZABETH JOHN, HARVEY J. SCHUGAR AND JOSEPH A. POTENZA

Department of Chemistry, Rutgers, The State University of New Jersey, New Brunswick, New Jersey 08903, USA

Abstract. [RuCl(NH$_3$)$_5$](HSO$_4$)$_2$.4H$_2$O, M_r = 487.88, triclinic, $P\bar{1}$, a = 10.0422 (5), b = 14.1044 (7), c = 6.3273 (6) Å, α = 100.369 (5), β = 98.655 (6), γ = 81.354 (4)°, V = 864.5 (3) Å^3, Z = 2, D_m = 1.86 (1), D_x = 1.874 g cm^{-3}, λ(Mo $K\alpha$) = 0.71073 Å, μ = 13.3 cm^{-1}, $F(000)$ = 498, T = 296 (1) K, R = 0.025 for 4622 unique reflections with $I > 3\sigma(I)$. The structure contains (NH$_3$)$_5$RuCl^{2+} cations, bisulfate anions and solvate water molecules all linked by an extensive hydrogen-bonding network. Each Ru ion is coordinated in a distorted octahedral fashion by five ammonia molecules and a chloride ion. The Ru—Cl distance [2.3742 (5) Å] is typical for Ru^{III}—Cl linkages. The Ru—NH$_3$ distances span a narrow range [2.096 (2)–2.119 (2) Å] and provide no evidence for a *trans* effect.

Introduction. For some time we have been interested in the ligand to metal charge-transfer spectra of pentaammineruthenium(III)L complexes, where L = thioether (Krogh-Jespersen, Zhang, Westbrook, Fikar, Nayak, Kwik, Potenza & Schugar, 1989) or imidazole (Krogh-Jespersen, Westbrook, Potenza & Schugar, 1987). Such complexes are prepared by reaction of (NH$_3$)$_5$Ru^{II}H$_2$O with an excess of the appropriate ligand, followed by air oxidation to the

Ru^{III} state. This intermediate in turn is prepared by the reduction of [(NH$_3$)$_5$RuCl]$^{2+}$ with zinc amalgam which is accompanied by rapid aquation of the initial [(NH$_3$)$_5$RuCl]$^+$ product. In an attempt to prepare the sulfate salt of (NH$_3$)$_5$Ru^{II}L, where L = 2, 4,6-trihydroxybenzoate, by a variation of a published procedure (Stritar & Taube, 1969), the addition of saturated aqueous (NH$_4$)$_2$SO$_4$ to an acidic solution which contained some unreacted [(NH$_3$)$_5$RuCl]$^{2+}$ precipitated this cation as its bisulfate salt. We report here the structure of this cation. A limited (R_F = 0.169, visually estimated intensities) early crystallographic study of the chloride analogue [(NH$_3$)$_5$RuCl]Cl$_2$ has been reported (Prout & Powell, 1962).

Experimental. The acidic reaction mixture noted above was layered over a saturated (NH$_4$)$_2$SO$_4$ solution in a test tube. After a week at room temperature, well formed rectangular plates showing a yellow, dark-yellow dichroism deposited. D_m was measured by flotation.

A yellow plate 0.15 × 0.30 × 0.32 mm crystal was mounted in a capillary and data collected using an Enraf–Nonius CAD-4 diffractometer with graphite-monochromated Mo $K\alpha$ radiation and θ–2θ scans. No systematic absences were observed. Cell con-